

Functionalization of Ti6Al4V Alloy with Polyphenols: The Role of the Titanium Surface Features and the Addition of Calcium Ions on the Adsorption Mechanism

*Original*

Functionalization of Ti6Al4V Alloy with Polyphenols: The Role of the Titanium Surface Features and the Addition of Calcium Ions on the Adsorption Mechanism / Reggio, C.; Barberi, J.; Ferraris, S.; Spriano, S.. - In: METALS. - ISSN 2075-4701. - 13:8(2023). [10.3390/met13081347]

*Availability:*

This version is available at: 11583/2981669 since: 2023-09-05T11:21:27Z

*Publisher:*

Multidisciplinary Digital Publishing Institute (MDPI)

*Published*

DOI:10.3390/met13081347

*Terms of use:*

This article is made available under terms and conditions as specified in the corresponding bibliographic description in the repository

*Publisher copyright*

(Article begins on next page)

## Article

# Functionalization of Ti6Al4V Alloy with Polyphenols: The Role of the Titanium Surface Features and the Addition of Calcium Ions on the Adsorption Mechanism

Camilla Reggio <sup>1</sup>, Jacopo Barberi <sup>1</sup> , Sara Ferraris <sup>1</sup>  and Silvia Spriano <sup>1,2,\*</sup> 

<sup>1</sup> DISAT Department, Politecnico di Torino, Corso Duca degli Abruzzi 24, 10129 Turin, Italy; camilla.reggio@polito.it (C.R.); jacopo.barberi@polito.it (J.B.); sara.ferraris@polito.it (S.F.)

<sup>2</sup> Centro Interdipartimentale Polito BioMEDLab, Politecnico di Torino, 10129 Turin, Italy

\* Correspondence: silvia.spriano@polito.it

**Abstract:** Functionalization of medical devices with biomolecules is a key strategy to control implant outcomes, for instance, polyphenols can produce fast osseointegration and reduce both the infection risk and inflammatory response. This paper is designed to evaluate the role of calcium ions and surface features in surface functionalization with a red pomace extract. An in-depth investigation of the binding mechanism between surfaces and polyphenols was also performed. A smooth Ti6Al4V alloy was used as a control substrate and compared with a bioactive and nanotextured chemical-treated Ti6Al4V alloy. Solutions with and without the addition of calcium ions were used for functionalization. The results showed that polyphenols were adsorbed in all cases, but in a larger amount in the presence of calcium ions. The functionalized surfaces were hydrophilic (contact angles in the range of 45–15°) and had isoelectric points at pH 2.8–3.1. The acidic hydroxyl groups on the chemically treated titanium alloy favored the chemisorption of complex compounds of flavonoids and condensed tannins with calcium ions, through a bridging mechanism, and made desorption sensitive to pH. On the smooth surface, the absence of reactive functional groups led to a lower amount of adsorbed molecules and a physisorption mechanism. Selective physisorption of phenolic acids was supposed to be predominant on the smooth surface in the presence of calcium ions in the solution.

**Keywords:** polyphenols; functionalization; titanium; chemisorption; physisorption



**Citation:** Reggio, C.; Barberi, J.; Ferraris, S.; Spriano, S. Functionalization of Ti6Al4V Alloy with Polyphenols: The Role of the Titanium Surface Features and the Addition of Calcium Ions on the Adsorption Mechanism. *Metals* **2023**, *13*, 1347. <https://doi.org/10.3390/met13081347>

Academic Editor: Dake Xu

Received: 6 July 2023

Revised: 21 July 2023

Accepted: 24 July 2023

Published: 27 July 2023



**Copyright:** © 2023 by the authors. Licensee MDPI, Basel, Switzerland. This article is an open access article distributed under the terms and conditions of the Creative Commons Attribution (CC BY) license (<https://creativecommons.org/licenses/by/4.0/>).

## 1. Introduction

The biomaterial surface is the locus of interaction between an implant and the biological environment. Surface features modulate the processes of water, ions, protein adsorption, cell adhesion, and tissue integration. This is why surface engineering and modification are key strategies for controlling the outcome of an implant and developing innovative materials [1]. The two main types of surface modifications are texturing of topography and functionalization. Functionalization is a chemical modification of biomaterials through a molecular layer of selected active compounds bounded to their surfaces [2]. The main advantage of functionalization in comparison to coatings is that it allows for coupling tailored surface texturing and chemical modification without masking the topography [3]. Moreover, the release from a functionalized surface usually occurs by breaking the bond of molecules with the surface and does not involve any degradation process as it occurs in the case of a resorbable coating carried with some active compounds, which can produce a variety of partially unpredictable products. The drawback of functionalization is that just a limited amount of active compounds can be linked to the surface and the release usually must overcome a concentration threshold to have substantial efficacy in the physiological environment [4].

The compounds for functionalization are selected according to specific targets, such as antibacterial action, fast osseointegration, modulation of the inflammatory response,

or multifunctional action [5,6]. The type of chemical bond between the molecules or compounds and the substrate is critical in determining the reproducibility of the process, rate of release, and biological response. A covalent chemical bond, as in the case of molecule grafting, guarantees a stable and long-lasting link with the surface, but the biological response can be hindered in the absence of a release in the surrounding biological fluids [7]. Conversely, physisorption is a weak chemical bond usually insufficient to guarantee reproducibility and a controlled kinetic release. Chemisorption is interesting for getting more controlled adsorption and desorption kinetics. A “smart release” of the adsorbed molecules can occur at a specific pH if electrostatic charges are involved in the chemical bond and they change with pH; this is of interest mainly for a targeted effect during the acute inflammatory response, at pH around 4.5 [2]. The chemical bond occurring at a functionalized surface is determined by the functional groups and charges of both the substrate and molecules to be linked. Pre-treatments of the substrate are often needed to make it suitable for functionalization and the parameters of the functionalization process (solvent, pH, temperature, and time) must be optimized to allow the chemical interaction with the substrate and molecules in the solution [8].

The strategy of this research was to use polyphenols of a natural extract to functionalize Ti6Al4V through adsorption. The challenging feature of these molecules is their multifunctional ability. They can reduce the risk of infection and modulate the inflammatory response with a chemical redox and radical scavenging action [9]. The advantage of a natural extract is that it is a mixture of different compounds with a synergic action [10]. A patented chemical treatment was performed on the substrate to obtain a hierarchically structured surface to promote osseointegration and surface adsorption ability [11,12]. Calcium ions were added to the functionalization solution to exploit the formation of complex compounds of polyphenols for chemisorption on the titanium substrate [9,13]. The specific goal of this research was the investigation of the role of calcium in the chemical bond of the polyphenols with the chemically treated titanium surface.

## 2. Materials and Methods

### 2.1. Sample Preparation

Grade 5 Ti6Al4V alloy was purchased as bars (10 mm in diameter—ASTM B348, Gr5, Titanium Consulting and Trading, Buccinasco, Italy). Disk-like samples (2 mm thick) were obtained through automatic cutting.

The reference specimens were polished using SiC polishing papers up to 4000 grit, washed in an ultrasonic bath once in acetone for 5 min, and finally twice in water for 10 min. Samples were dried under a laminar-flow hood. These samples are referred to as Ti64.

The surface chemical treatment was described in previous work [11]. Briefly, Ti64 disks were gritted with #400 SiC sandpaper, washed as before described, etched in hydrofluoric acid (Sigma-Aldrich, St. Louis, MO, USA), and finally treated in hydrogen peroxide (PanReac AppliChem, Darmstadt, Germany). The surface-treated samples are called CT.

### 2.2. Functionalization with Polyphenols

Functionalization of Ti64 and CT samples was obtained by soaking them in polyphenols solutions. Polyphenols were extracted from Barbera grape pomaces and lyophilized through a protocol implemented in previous work [9,14].

Two different functionalization solutions were prepared. The first one was obtained by dissolving the extract in a buffered solution, prepared by adding 39 mL/L of HCl and 6.188 g/L of Tris(hydroxymethyl)aminomethane (TRIS—Sigma Aldrich, St. Louis, MO, USA) to ultrapure MilliQ water, following this order. This buffered solution was denoted as TRIS/HCl and had pH = 7.4. The second solution was made in the same way with the preliminary addition of 0.292 g/L of CaCl<sub>2</sub> (Sigma Aldrich, St. Louis, MO, USA). This solution is referred to as TRIS/HCl+Ca.

Polyphenols were added to TRIS/HCl and TRIS/HCl+Ca solutions in a concentration equal to 5 mg/mL and stirred for 1 h to completely dissolve polyphenols. The obtained solutions are called TRIS/HCl\_P and TRIS/HCl+Ca\_P, respectively.

Before functionalization, Ti64 and CT samples were exposed for 1 h to UV light (UV-C 40 W; 253.7 nm). In this way, carbonaceous contaminations on the samples were removed and specimen surfaces were activated. The functionalization step was obtained by soaking the samples in 5 mL of TRIS/HCl\_P or TRIS/HCl+Ca\_P solutions for 3 h at 37 °C in dark conditions. After that, the samples were gently rinsed in MilliQ water, dried under a laminar flow hood, and stored in dark conditions. Functionalized samples are denoted as Ti64\_P and CT\_P when the TRIS/HCl\_P solution was used, or Ti64\_P\_Ca and CT\_P\_Ca when the TRIS/HCl+Ca\_P solution was employed for functionalization.

The chemical and physical characterization of the control and modified surfaces was performed using XPS, fluorescent microscopy, AFM with Kelvin probe, wettability, and zeta potential measurements.

### 2.3. X-ray Photoelectron Spectroscopy (XPS)

XPS survey and high-resolution (HR) spectra were acquired on all the samples to investigate the surface chemistry (PHI 5000 Versaprobe II, ULVAC-PHI, Inc., Kanagawa, Japan). The source was Al-K and the take-off angle was set at 45°. HR measures were performed in the region of carbon C1s and oxygen O1s. An eventual charging effect was compensated by setting the C1s peak at 284.80 eV [15]. Peak deconvolution of the HR spectra was performed using the software CasaXPS [16] by applying a Shirley background and a Gaussian-Lorentzian (70–30%) line shape [17,18].

### 2.4. Fluorescent Imaging

The natural polyphenols' fluorescence was exploited to image their distribution on the surface of the samples [9,14]. An optical microscope (LSM 900, ZEISS, Oberkochen, Germany) was employed with a fluorescent light source and with a red filter [19] (emission: 573 nm), setting the exposure time to 1s and magnification of 200× for each image.

### 2.5. Kelvin Probe Force Microscopy

Kelvin probe force microscopy (KPFM) was employed to investigate the distribution of polyphenols on the surfaces of the titanium samples. KPFM was previously adapted by the authors to observe organic molecules on titanium surfaces [18,20]. Briefly, Ti64 and CT samples were half-masked with Kapton® tape and subsequently functionalized with the different solutions, as described in paragraph 2.2. When the samples were dried, the tape was removed and KPFM imaging was performed on the edge of the masked area, with an atomic force microscope (Innova, Bruker, Billerica, MA, USA) equipped with conductive diamond tips (AD-2.8-AS, Adama Innovations LTD., Dublin, Ireland). A second-degree polynomial filter was applied to the topographical images, while the matching alignment method was employed for the electric potential images using the Gwyddion software [21].

### 2.6. Water Contact Angle

Surface wettability was assessed through water contact angle (WCA)  $\theta$  with the sessile drop method (FTA 1000C, MP instrument, Bussero, Italy). Both Ti64 and CT specimens were tested before and after functionalization in the two different solutions. Results are expressed as the average value measured on three different measures, plus minus standard deviation.

### 2.7. Zeta Potential

The zeta potential was measured both on polyphenols in the functionalization solutions and on the surface of the samples. For the determination of the zeta potential of suspended polyphenols in the solutions, a dynamic light scattering system was used (Litesizer 500, Anton Paar, Gratz, Austria). As the electrolyte, KCl was added to both

TRIS/HCl\_P and TRIS/HCl+Ca\_P solution, to obtain a concentration of 1 mM. Titration curves were obtained by manually titrating the pH with 0.05 M NaOH or 0.05 M HCl.

The zeta potential of solid samples was obtained by an electrokinetic analyzer mounting an adjustable gap cell (SurPASS, Anton Paar, Gratz, Austria) on all the samples. Zeta potential values were measured by fluxing an electrolyte solution (0.001 M KCl) within the cell, mounting a couple of samples separated by a gap about 100  $\mu\text{m}$  wide. Titration curves of specimens were obtained by automatic titration of the electrolyte solution. NaOH and HCl 0.05 M were used for the basic and acid range, respectively. A different pair of samples was used for each range. XPS was also performed on Ti64\_P\_Ca\_pza and CT\_P\_Ca\_pza, which are the Ti64\_P\_Ca and CT\_P\_Ca samples used for the titration in the acidic range. The stability of the functionalization layer was also tested using zeta potential at a constant pH. The electrolyte solution was manually titrated at a pH value equal to  $4.0 \pm 0.1$  or  $7.4 \pm 0.1$ . Subsequently, zeta potential was measured over a period of about 100 min. During the measurement, the samples were subjected to an almost continuous flux of the electrolyte solution.

### 2.8. Statistical Analysis of the Data

Statistical analysis of the wettability data was performed through ANOVA one-way test, the significance level tested are  $p < 0.05$ ,  $p < 0.01$ , and  $p < 0.001$ . Finally, Turkey's multiple comparison tests were performed to detect significant differences between samples.

## 3. Results

### 3.1. X-ray Photoelectron Spectroscopy

The elemental composition of the surfaces was measured by X-ray photoelectron spectroscopy and the results are reported in Table 1. The presence of adventitious carbon contamination on Ti64 and CT is unavoidable and it was expected even if surface decontamination was performed by UV exposition [9]. The ratio of the carbon and oxygen percentages changed after functionalization with polyphenols (Ti64\_P and Ti64\_P\_Ca vs. Ti64; CT\_P and CT\_P\_Ca vs. CT), with an increase in carbon and a decrease in oxygen in comparison with both substrates. This was the first qualitative evidence of the effectiveness of the functionalization process considering the organic nature and high carbon content of polyphenols and the high content of oxygen of the oxide layer on titanium surfaces. A semi-quantitative evaluation of the amount of adsorbed polyphenols was obtained by calculating the C/O ratio. The largest C/O ratios were recorded on Ti64\_P\_Ca and CT\_P\_Ca evidencing a positive effect on the adsorption of the addition of calcium ions to the functionalization solution. The opposite trend was observed for titanium, which was progressively reduced by moving from Ti64 to Ti64\_P and Ti64\_P\_Ca, as well as from CT to CT\_P and CT\_P\_Ca.

**Table 1.** Surface chemical composition (at %) of the samples before and after functionalization from XPS survey analysis.

| Samples       | Elements [at %] |       |       |      |      |     |        |      |
|---------------|-----------------|-------|-------|------|------|-----|--------|------|
|               | C               | O     | Ti    | N    | Al   | Ca  | Others | C/O  |
| Ti64          | 23.55           | 51.84 | 16.36 | 3.39 | 3.62 | -   | -      | 0.45 |
| Ti64_P        | 54.6            | 27.4  | 4.6   | 2.8  | -    | -   | -      | 1.99 |
| Ti64_P_Ca     | 69.8            | 27.3  | 0.3   | 1.8  | -    | 0.2 | 0.6    | 2.56 |
| Ti64_P_Ca_pza | 62.7            | 29.7  | 1.6   | 1.4  | -    | 0.4 | 4.2    | 2.11 |
| CT            | 12.1            | 62.9  | 21    | 2.52 | 2.4  | -   | 1.6    | 0.19 |
| CT_P          | 53              | 38.9  | 6.5   | 1.5  | -    | -   | -      | 1.36 |
| CT_P_Ca       | 62.6            | 30.1  | 1.2   | 3    | -    | 1.3 | 1      | 2.08 |
| CT_P_Ca_pza   | 55.7            | 36.6  | 5.1   | 2.3  | -    | 0.1 | 0.2    | 1.52 |

Calcium was revealed in a higher quantity on CT\_P\_Ca vs. Ti64\_P\_Ca evidencing a higher ability of CT to adsorb positive ions from the solution. This agreed with the bioactive

behavior of this surface, which is the ability to induce the precipitation of hydroxylapatite from a simulated body fluid solution in which the first step is the adsorption of calcium ions from the solution [22]. A limited (0.2–0.8 %) adsorption of calcium occurred also on Ti64\_P and CT\_P because of a small content of calcium in the polyphenols extract [9]. The samples Ti64\_P\_Ca\_pza and CT\_P\_Ca\_pza (obtained after the acidic zeta potential titration of Ti64\_P\_Ca and CT\_P\_Ca, see Section 3.5) showed an amount of adsorbed polyphenols, respectively, between Ti64\_P\_Ca and Ti64\_P or CT\_P\_Ca and CT\_P according to the carbon and titanium amounts. In the case of CT\_P\_Ca\_pza, there was a significant reduction of calcium in comparison to CT\_P\_Ca. These results showed the removal of polyphenols during titration in the acidic range, as discussed in Section 4.

The high-resolution analysis of the XPS peaks (Figure 1–Table 2) was used to define the type of polyphenols and their mechanism of adsorption on the surfaces. Considering the O1s region, the peaks at 530.6–529.9 and 530.8–531.0 eV were assigned, respectively, to the Ti-O bond and acidic OH functional groups (acOH) [11,22]. After functionalization, there was a significant decrease in the Ti-O peak, as expected. The reduction was greater in the samples functionalized with calcium ions on both substrates. These data confirmed larger adsorption of polyphenols by using calcium ions as a linker. The acOH peak on CT was high due to the great density of this functional group on the titanium oxide layer induced by the chemical etching here used. After functionalization, a contribution from acidic OH groups of polyphenols to this peak was expected and the ratio between the Ti-O and acOH peaks was lower after functionalization than it was on CT.

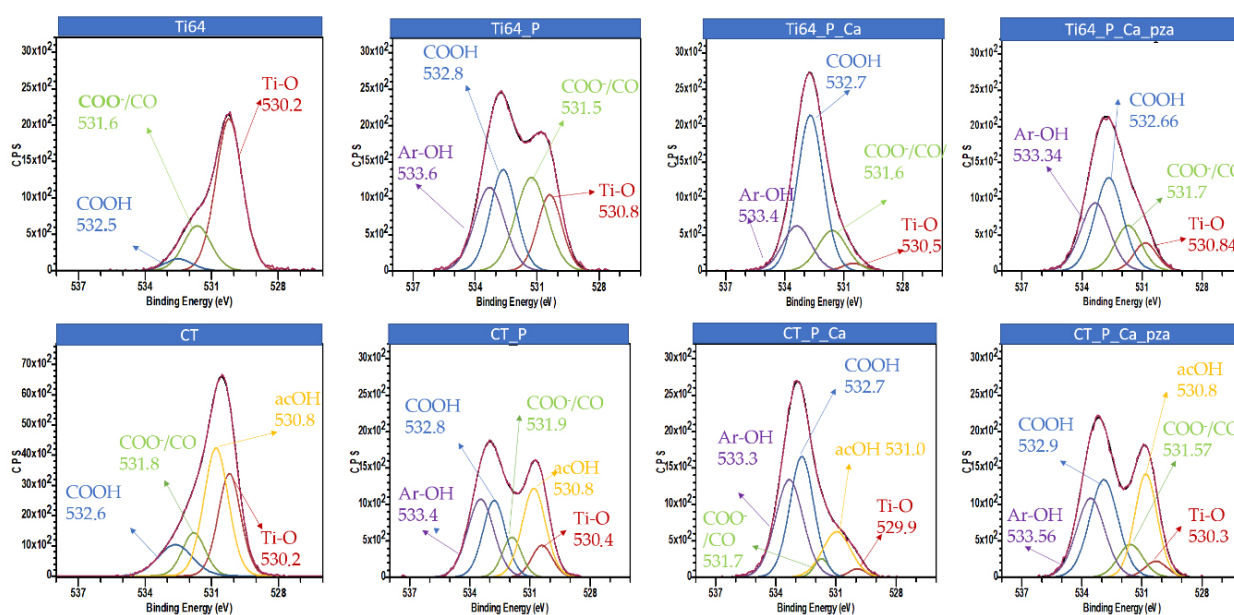


**Figure 1.** High-resolution spectra of O 1s region of Ti64, Ti64\_P, Ti64\_P\_Ca, Ti64\_P\_Ca\_pza, CT, CT\_P, CT\_P\_Ca, and CT\_P\_Ca\_pza samples.

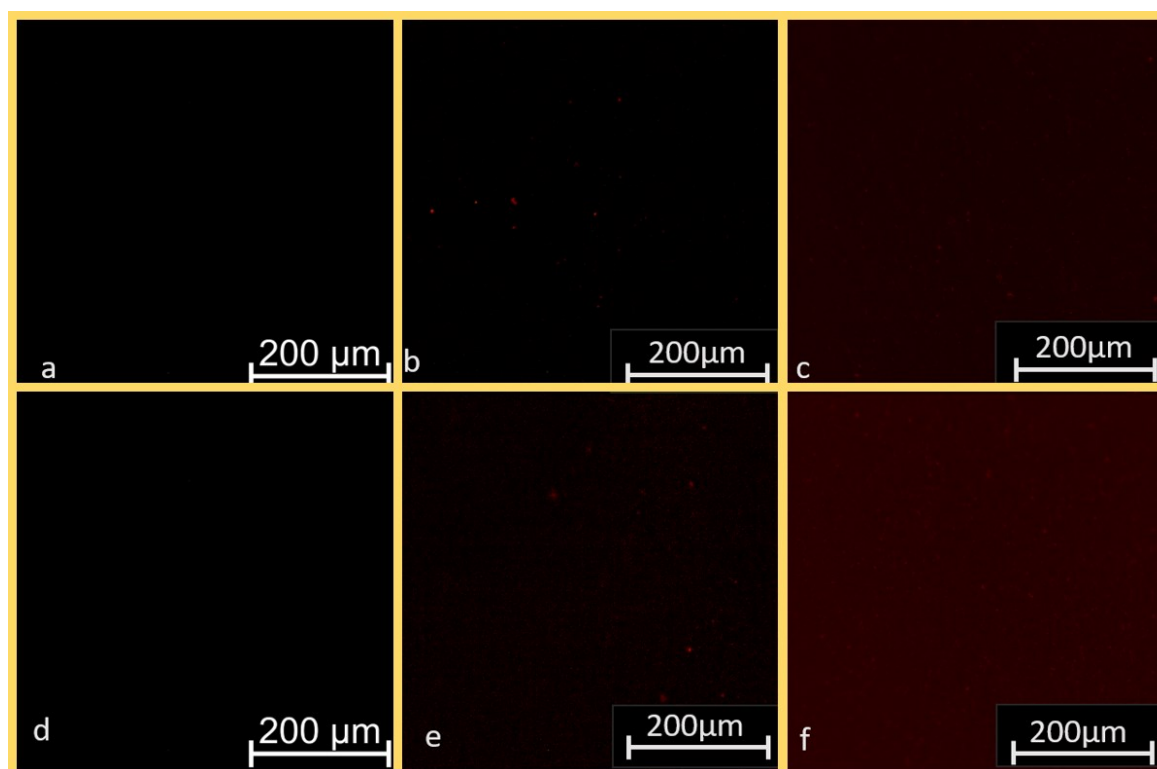
The peaks at 531.3–531.8 eV were assigned to the functional groups COO<sup>-</sup> or CO or OH with basic behavior and the peaks at 533.3–533.4 to ArOH groups [14,18,23]. The COOH was assigned to 532.5–532.7 eV, in the literature it could be attributed to adsorbed water (adsH<sub>2</sub>O), but this attribution did not seem reasonable [9,12,24]. A small contribution from basic OH groups can be expected only from the substrate Ti64 [25]. The peaks of Ar-OH and COOH, respectively, appeared or increased after functionalization with polyphenols on both substrates, both with and without the presence of calcium ions in the solution. The ratio COOH/Ar-OH increased on Ti64\_P\_Ca vs. Ti64\_P and CT\_P\_Ca vs. CT\_P, largely on Ti64\_P\_Ca vs. CT\_P\_Ca. The contribution of the peak related to COO<sup>-</sup> or CO was minimum on CT\_P\_Ca and progressively increased on CT\_P, and Ti64\_P or Ti64\_P\_Ca. A detailed discussion of these data is reported in Section 4.

**Table 2.** Component assignment and percentage composition of each component of the high-resolution spectra of the oxygen region. Data related to adventitious contaminations are reported in brackets.

| Samples       | Components O1s Region [%] |       |                      |         |       |            |
|---------------|---------------------------|-------|----------------------|---------|-------|------------|
|               | Ti-O                      | acOH  | COO <sup>-</sup> /CO | COOH    | ar-OH | COOH/ar-OH |
| Ti64          | 71.87                     | -     | (22.21)              | (5.92)  | -     | -          |
| Ti64_P        | 9.92                      | -     | 16.37                | 45.43   | 28.27 | 1.6        |
| Ti64_P_Ca     | 2.81                      | -     | 17.82                | 60.13   | 19.25 | 3.1        |
| Ti64_P_Ca_pza | 10.7                      | -     | 18.75                | 40.54   | 30.64 | 1.3        |
| CT            | 30.74                     | 41.88 | (13.13)              | (14.25) | -     | -          |
| CT_P          | 9.01                      | 28.79 | 10.52                | 23.63   | 28.04 | 0.8        |
| CT_P_Ca       | 2.03                      | 17.65 | 3.72                 | 39.71   | 36.89 | 1.1        |
| CT_P_Ca_pza   | 4.23                      | 27.23 | 9.65                 | 32.61   | 26.28 | 1.2        |

### 3.2. Fluorescent Imaging

The polyphenol natural fluorescence can be exploited to visualize the distribution of the molecules adsorbed on the different surfaces (Figure 2). CT and Ti64 surfaces had no intrinsic fluorescence (Figure 2a–d) while a uniform fluorescent layer was observed on CT\_P\_Ca, CT\_P, and Ti64\_P\_Ca (Figure 2c–f). The intensity of the fluorescent signal was the highest on CT\_P\_Ca. In contrast, only isolated spots are visible on Ti64\_P (Figure 2b). These images were used for a qualitative evaluation of the amount of adsorbed molecules, but it must be considered that the fluorescence signal cannot be visualized below a certain threshold and this technique can fail in imaging a thin layer of fluorescent molecules.

**Figure 2.** Fluorescence microscopy images of (a) Ti64 (b) Ti64\_P, (c) Ti64\_P\_Ca, (d) CT, (e) CT\_P, (f) CT\_P\_Ca.

### 3.3. AFM Surface Topographical and Electric Potential Imaging

The distribution of polyphenols could be observed at larger magnification than fluorescent microscopy thanks to KPFM topographical imaging. The results are reported in Figure 3.

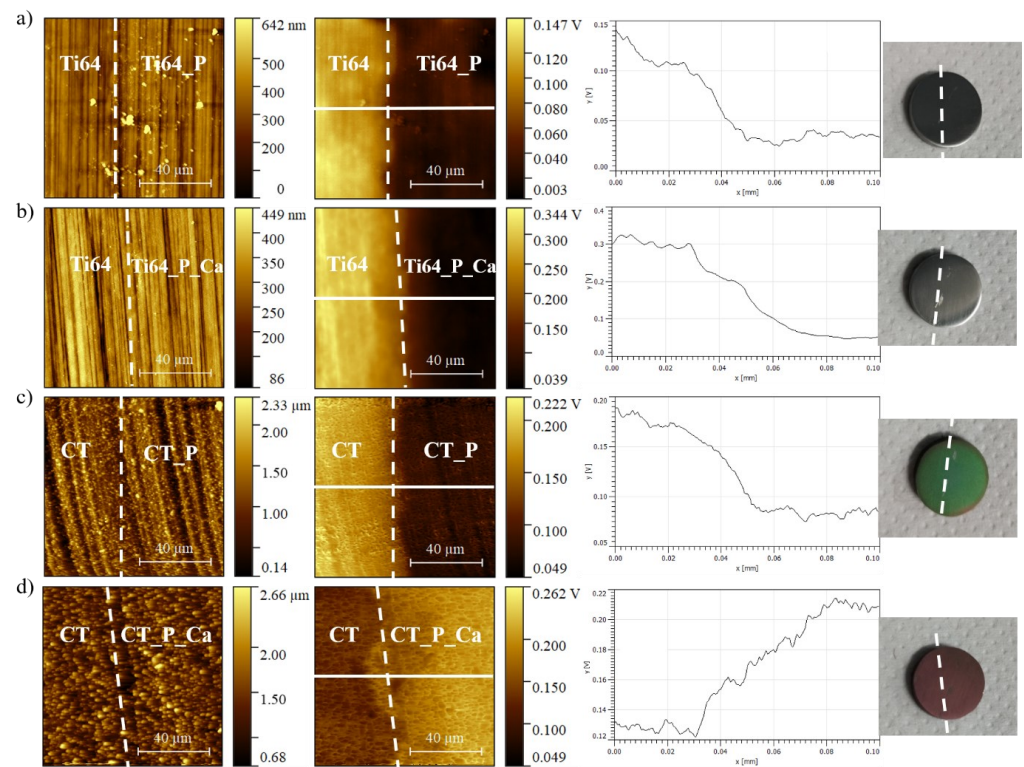


**Figure 3.** Topographical (first column) and surface potential images (second column), profile (third column), and photo (fourth column) of samples half covered by polyphenols: (a) Ti64\_P; (b) Ti64\_P\_Ca; (c) CT\_P; (d) CT\_P\_Ca. The areas without (on the left) and with (on the right) polyphenols are separated by a dashed line. The electric potential profile was evaluated along the continuous horizontal line of the second column.

The expected surface morphology of Ti64 and CT samples can be seen in the topographical images (Figure 3). Ti64 was mainly flat and characterized by polishing grooves, while CT showed the expected micro-structure of the nano-porous oxide layer, in which the titanium beta grains raise from the bulk due to selective etching by HF during the chemical treatment [26]. The nanopores cannot be seen at this scale with the AFM. The adsorbed polyphenols were not visible in the topographical images. Some aggregates were found only on Ti64\_P in agreement with the fluorescence images. The presence of a continuous layer following the topography of the substrates could be supposed on Ti64\_P\_Ca, CT\_P, and CT\_P\_Ca according to these images, fluorescence images, and XPS results.

Different information could be derived from the electric potential images. Firstly, they highlighted the presence of the adsorbed molecules, thanks to a difference in the surface electric potential of the functionalized sample area. On Ti64\_P, Ti64\_P\_Ca, and CT\_P the areas functionalized with polyphenols were uniformly at a lower electric potential than the substrates (sample areas not functionalized are on the left of the images), as it is common in the case of organic molecules on titanium surfaces [18,20]. The negative differences between the two areas were about 100–250 mV on these samples. Contrary, on the CT\_P\_Ca sample, the functionalized area had a higher electric potential than the substrate (CT), with a positive difference of about 80 mV.

### 3.4. Water Contact Angle

The water contact angle is sensitive to the chemistry of the surface, so it is useful to assess chemical modifications on surfaces and functionalization with organic molecules; the obtained values are reported in Figure 4. The reported values are the apparent contact angles without considering the roughness of the samples. The Sa values of these surfaces



are close to 0.1 microns and the correction due to roughness does not substantially affect the data [27].

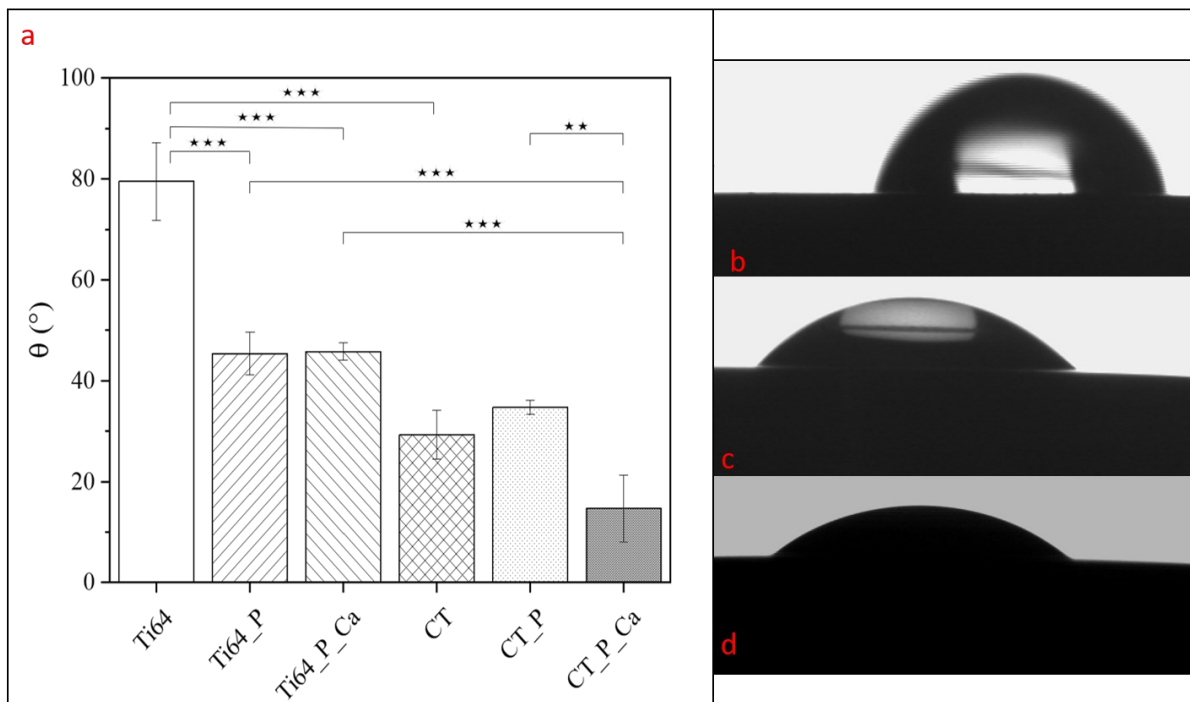


**Figure 4.** (a) Water contact angle ( $\theta$ ) on all the investigated surfaces. Bars represent the standard deviations. Stars represent the significance level: \*\* =  $p$ -value < 0.01, \*\*\* =  $p$ -value < 0.001; (b–d) Photos of water droplets on Ti64, Ti64\_P, and CT\_P\_Ca, respectively.

Polished titanium (Ti64) had the highest value of  $\theta$  ( $81.4 \pm 0.77^\circ$ ) in agreement with the literature [28]. As already reported by the authors [11], the chemical treatment produces a significantly more hydrophilic surface (CT), with a contact angle of  $28.4 \pm 4.2^\circ$ , due to the presence of nano-topography and hydroxyl groups. The functionalization with polyphenols can increase the hydrophilicity of both types of surfaces, depending on the presence of calcium ions. In the case of Ti64\_P and Ti64\_P\_Ca, the wettability was similar ( $\theta \approx 45^\circ$ ) but statistically different from Ti64 ( $p$ -value < 0.001). Compared to the CT surface, CT\_P and CT\_P\_Ca showed no significant variation. Furthermore, the CT\_P\_Ca resulted in the most wettable surface after functionalization with a contact angle of  $14.7 \pm 6.6^\circ$ , which was significantly lower than the one of CT\_P ( $p$ -value < 0.01), Ti64\_P\_Ca, and Ti64\_P ( $p$  value < 0.001).

### 3.5. Zeta Potential Titration Curves

The zeta potential is related to the surface charge and its variation by changing the pH of the electrolyte provides information about the acidic or the basic nature of functional groups on the surface of a bulk sample or colloidal particles. The titration curves obtained on polyphenols in TRIS/HCl\_P and TRIS/HCl+Ca\_P (Figure 5) are already reported and discussed in previous work by the authors [9] and are here used as a reference. The zeta potential titration curves of all the investigated samples are reported in Figure 5a,b.

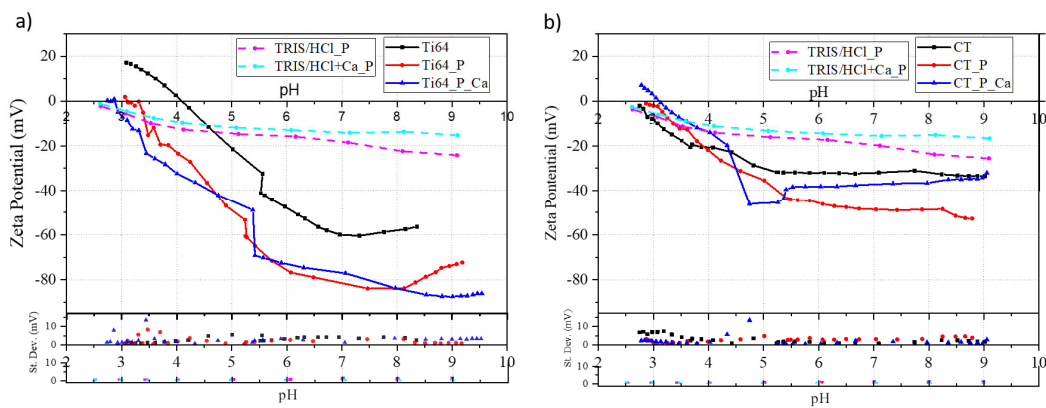


**Figure 5.** Surface zeta potential vs. pH curves of (a,b) polyphenols in solution, without (TRIS/HCl\_P) and with (TRIS/HCl+Ca\_P) the addition of calcium ions, and of samples before and after functionalization with both the solutions on Ti64 (a) or CT (b) substrates. Standard deviations are reported in the underneath graphs.

The solubilized polyphenols had a negative zeta potential independently of the pH and the eventual addition of calcium ions (Figure 4a). The isoelectric points (IEP) were not measured in the explored pH range, but their values can be extrapolated, falling around pH 2.0–2.2 in both cases, without an effect of the presence of calcium ions. The TRIS/HCl\_P and TRIS/HCl+Ca\_P solutions had very similar zeta potential values in the range of pH 2.5–7 with a small variation of the slope of the curve around pH 4. At pH 7, the zeta potential of TRIS/HCl+Ca\_P had a plateau at around  $-15$  mV, while TRIS/HCl\_P continued with a progressive reduction of the zeta potential by increasing pH. In both cases, the standard deviations of the zeta potential were very low.

The zeta potential titration curves of Ti64 and CT were greatly different (Figure 5b,c). As deeply discussed in previous work [25], this is due to the generation of very strong acidic OH groups on CT during the hydrogen peroxide treatment, while Ti64 does not expose a prevalence of functional groups with an acidic or basic behavior, as deduced by the IEP detected at pH 4 and the absence of any plateau. The acidic OH groups exposed by the titanium oxide layer on CT are completely deprotonated at any pH higher than 4, which is the onset of the plateau in the basic range and induced a substantially lower IEP, down to pH 2.6.

Furthermore, the functionalization with polyphenols resulted in a change in the zeta potential compared to the substrates. In the case of the polished samples (Figure 5b), the overall zeta potential was lower on both Ti64\_P and Ti64\_P\_Ca if compared to Ti64, being around 20 mV more negative over the full pH range and the IEPs shifted from 4 to 3 and 2.8, respectively. The shift of the IEPs was toward lower pH values, getting close to the IEPs of functionalization solutions. All the observed differences between the titration curves of Ti64\_P and Ti64\_P\_Ca vs. Ti64 agreed with the presence of adsorbed polyphenols on the surface: the acidic OH groups of polyphenols caused a shift of the IEPs and lower zeta potential values. The presence of calcium ions in the functionalization solution did not substantially affect the zeta potential titration curves in the case of Ti64 as substrate. A small gap between the first points of the acid and basic titration range can be observed at pH 5.5 both on Ti64\_P and Ti64\_P\_Ca but it can be considered within the experimental error of this technique. Some small variations of the standard deviation of the zeta potential could be observed at low pH but they did not match with any evident change in the titration curves and can be considered within the experimental error of the techniques or related to some limited effect of the release of molecules from the surfaces.

Considering the chemically treated and functionalized surfaces (Figure 5c), the effects due to functionalization on the zeta potential were different. The IEPs were shifted to the right from pH 2.6, which was the IEP for CT, to 2.8 for CT\_P and 3.1 for CT\_P\_Ca. In this case, the shift was not in the direction of the IEPs of the functionalization solutions but in

the opposite one (toward higher pH values): this phenomenon will be explained in the discussion (Section 4). In the basic range, the curves of CT and CT\_P\_Ca had a similar plateau at about  $-30$  mV, while CT\_P showed a plateau at a more negative zeta potential value ( $-50$  mV). The presence of an evident and abrupt change in the zeta potential occurred at pH 4 in the case of CT\_P\_Ca: it was larger than 20 mV and did not occur at the first points of the acidic or basic titrations, so it cannot be considered as an experimental error. An evident larger standard deviation of the zeta potential was also visible at the same point. These phenomena can be correlated to an abrupt change in the surface chemistry and, in this case, to the release of some molecules.

The sample surface stability was tested by measuring the zeta potential for 100 min at fixed pHs, particularly at the inflammatory (pH 4) and physiological (pH 7.4) ones (Figure 6) [28].

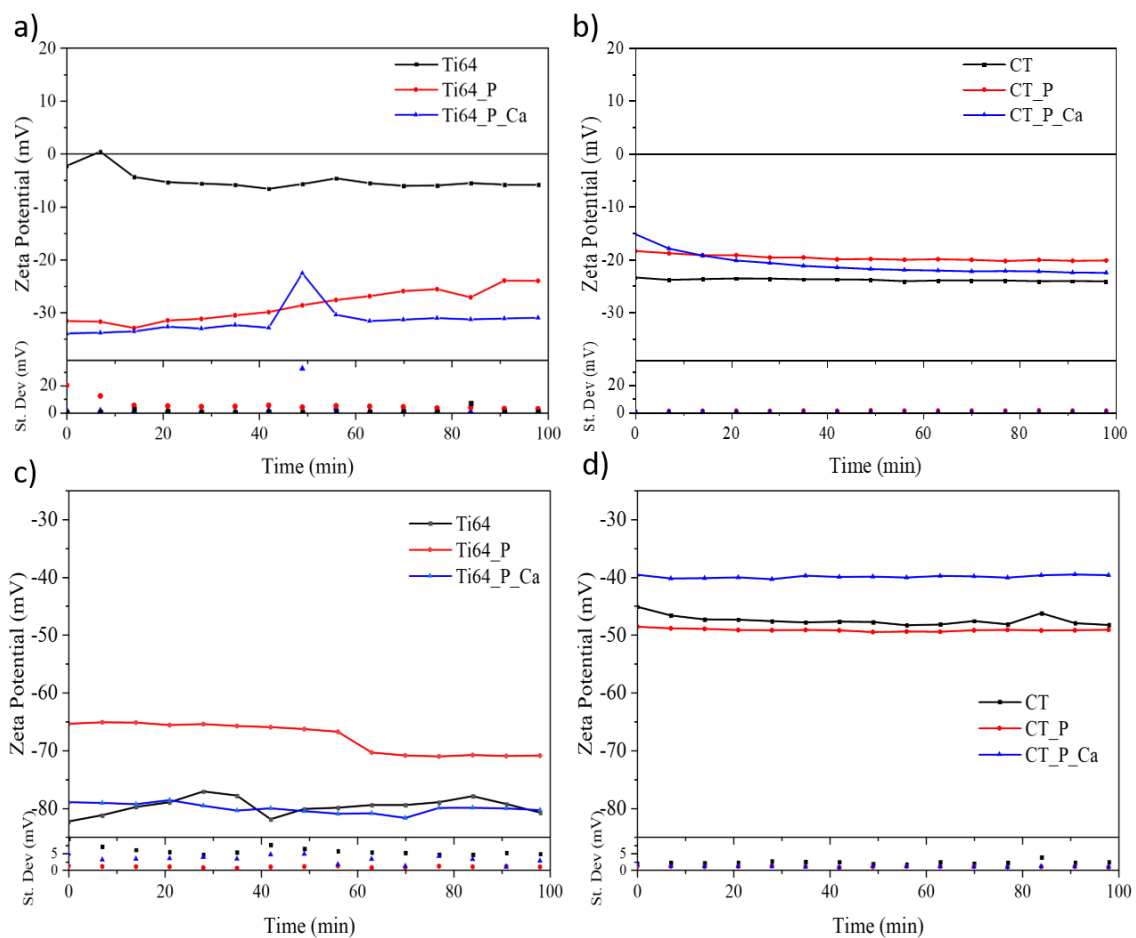


**Figure 6.** Plot of the zeta potential versus time at constant pH of all the investigated surfaces: (a,b) pH = 4; (c,d) pH = 7.4. Standard deviations are reported in the underneath graphs.

In most of the cases, the observed zeta potential values were almost constant and close to the ones reported at the corresponding pH in the titration curves (Figure 5), falling in the instrument's sensitivity range of about 10 mV. A trend toward a lower zeta potential can be observed in the first 20 min of the measurement on CT\_P\_Ca at pH 4.

#### 4. Discussion

The use of natural polyphenols for functionalizing or coating bioactive surfaces has been already investigated by the authors on chemically treated titanium, bioactive glasses, and hydroxylapatite [10,23]. Polyphenols can be linked to CT maintaining their anti-oxidant and radical scavenging ability [9] and they can increase the osteoblast differentiation and

mineralization of osteoblastic cells [29]. Here, the role of the surface features of the titanium substrates and bonding mechanisms were analyzed more in detail by comparing untreated and chemically treated titanium substrates in addition to the presence or not of calcium ions in the functionalization solution (Ti64\_P vs. Ti64\_P\_Ca; CT\_P vs. CT\_P\_Ca).

Polyphenols were adsorbed both on Ti64 and CT with or without the addition of calcium ions to the functionalization solution according to the XPS data (Tables 1 and 2, Figure 1), fluorescence (Figure 2), and KPFM (Figure 3) images, contact angle values (Figure 4), and zeta potential titration curves (Figures 5 and 6). Apart from this general observation, some differences due to the surface features of the substrates and the chemical composition of the functionalization solutions can be observed.

The XPS data (Figure 1) and fluorescence images (Figure 2) suggested that the addition of calcium ions to the functionalization solution increased the amount of adsorbed polyphenols on both substrates. When calcium was added to the functionalization solution, a higher ratio of C/O (Table 1), a lower contribution of the chemical bond Ti-O and functional group aCOH coming from the substrates (Table 2), and a stronger fluorescence signal (Figure 2) were detected compared with the adsorption without calcium. In the case of Ti64 substrates, the amount of calcium detected by XPS on Ti64\_P\_Ca (Table 1) was very low, so no effect related to the adsorption of calcium ions or chemical compounds with calcium can be supposed. The increase in the quantity of adsorbed polyphenols on Ti64\_P\_Ca vs. Ti64\_P could be explained by a change in the solubility of polyphenols by changing the ionic strength of the solution (because of the addition of the calcium salt) and because of the formation of complex compounds between calcium ions and some species of polyphenols in the solution: this hypothesis will be better described in the following. In the case of CT substrates, an evident presence of calcium was observed on CT\_P\_Ca by XPS (Table 1) and the higher adsorption of polyphenols during functionalization in TRIS/HCl+Ca\_P could be ascribed to a different mechanism of adsorption, involving the chemisorption of calcium ions on the titanium surface, as explained in the following.

The mechanism of adsorption is here discussed by using all the data acquired in this paper in a complementary way. First of all, the phenomena occurring in the functionalization solutions were considered. The grape extract here used contained phenolic acids (hydroxycinnamic and/or hydroxybenzoic), flavonoids, and condensed tannins [9]. The zeta potential titration curves of the functionalization solutions (Figure 5) underlined the presence of two types of hydroxyl groups in the polyphenols extract: one was a stronger acid and it was completely deprotonated at pH 4 while the other one was weaker and fully deprotonated only at pH 7. According to the literature, the first one can be associated with the carboxylic group of phenolic acids such as hydroxycinnamic acids [30], and the second one with the phenolic group typical of flavonoids and condensed tannins. The formation of complex compounds occurred when calcium ions were added to the functionalization solution and it involved the phenolic groups, slightly changing the zeta potential titration curve of TRIS/HCl+Ca\_P vs. TRIS/HCl\_P at basic pH values. It could be supposed that mainly flavonoids and condensed tannins were involved in the formation of the complex compounds considering that the change in the zeta potential titration curve of TRIS/HCl+Ca\_P involved mainly the plateau at pH 7 that was related to the phenolic groups of these compounds. The phenolic group of hydroxybenzoic acids is usually reported as completely deprotonated only at higher pH (around 8.5) but its involvement in the formation of complex compounds with calcium ions cannot be excluded. The formation of complex compounds with some species of polyphenols induces a higher solubility of those species, as it is reported in the literature [31]. According to this, the adsorption of different species of polyphenols on the substrates could be supposed when the functionalization occurred in TRIS/HCl\_P or TRIS/HCl+Ca\_P, as described in the following.

Considering the features of the substrates, Ti64 did not show any prevalence of hydroxyl groups with a strongly acidic or basic behavior, according to the zeta potential titration curve (Figure 5), and a low contribution of electrostatic interactions can be supposed on this surface during the adsorption of polyphenols even with the addition of

calcium ions to the functionalization solution. The data obtained showed a low amount of calcium in Ti64\_P\_Ca (Table 1), confirming this hypothesis.

On the other side, there was a net prevalence of deprotonated acidic hydroxyl groups on CT when the functionalization occurred at pH 7.4 [22,27,32]. A strong electrostatic contribution could be supposed during functionalization on CT. This was confirmed by the high amount of calcium detected by XPS on CT\_P\_Ca (Table 1). The larger adsorption of polyphenols on CT\_P\_Ca vs. CT\_P could be explained by the adsorption of the complex compounds of polyphenols with calcium ions and the bridging effect of the divalent ions. It has been acknowledged that divalent positive ions can act as bridges between negatively charged biomolecules, such as proteins, and negative surfaces [32,33]. The same effect was observed by the authors in a previous work involving CT as a substrate [9]. The contribution of the peak related to the acOH groups (Figure 1–Table 2) was lower on CT\_P\_Ca than on CT\_P in agreement with the hypothesis of the involvement of this functional group of the substrate in the chemisorption of the adsorbed layer through the mediation of calcium ions. Moreover, the shift toward higher pH values of the IEPs of CT\_P and CT\_P\_Ca compared to CT (Figure 5) can be explained by the progressive engagement of the acidic OH groups typical of CT by the adsorbed layer of polyphenols and/or their involvement in the chemisorption of calcium ions. The bridging effect was not observed on Ti64 due to the low availability of binding sites on the untreated titanium alloy.

The addition of calcium ions to the solution induced the adsorption of polyphenols with a largely enhanced exposition of COOH species than Ar-OH on Ti64: the COOH/Ar-OH ratio was 1.6 on Ti64\_P while it became 3.1 on Ti64\_P\_Ca (Figure 1 and Table 2). This can be explained as follows. The formation of complex compounds of calcium ions with polyphenols occurred through the Ar-OH functional groups of flavonoids and condensed tannins, as before mentioned. In the case of Ti64\_P\_Ca, the complex compounds with calcium ions were not bound by the substrate, because of the low density of deprotonated OH groups on Ti64 (Figure 5) and the resulting low attraction of calcium ions. Consequently, higher adsorption of other species, such as phenolic acids can be supposed. A physisorption mechanism of phenolic acids was supposed to be predominant in the case of Ti64\_P\_Ca. In the case of CT substrates, the presence of a high density of negative charge on CT, due to deprotonated OH groups of the oxide layer (Figure 5), may change the adsorption mechanism mainly to chemisorption, with a strong effect of electrostatic interactions. In the case of CT\_P\_Ca, there was a reduced exposition of the COO<sup>-</sup> groups compared to Ti64\_P, Ti64\_P\_Ca, and CT\_P (Figure 1–Table 2). These groups were electrostatically repulsed by the substrate (Table 2 and Figure 1), agreeing with the hypothesis of chemisorption. With the addition of calcium ions to the solution, the ratio between COOH/Ar-OH on CT\_P\_Ca was increased compared to CT\_P because in this case the phenolic groups of the adsorbed species were used for the formation of the complex compounds with calcium ions (Table 2 and Figure 3) and were not exposed: this also agreed with the hypothesis of chemisorption of complex compounds of flavonoids and tannins with calcium ions on CT.

Looking at the wettability (Figure 4) and zeta potential titration curves (Figure 5), comparable contact angle and zeta potential titration curves were detected on Ti64\_P and Ti64\_P\_Ca. This highlights that the surface chemistry of these samples was analogous, independently from the addition of calcium ions, and that there was an overall limited effect of the addition of calcium ions to the functionalization solution in the case of Ti64.

In contrast, the addition of calcium ions to the functionalization solution of CT resulted in surfaces with different features compared to the other samples here considered. CT\_P\_Ca showed a higher wettability than CT\_P and the other functionalized samples (Figure 4), in agreement with a substantial effect of the added calcium ions, which leads to a higher amount of adsorbed polyphenols and different species of them on the titanium surface.

Lastly, the data from KPFM (Figure 3) confirmed a substantial difference in the adsorption of polyphenols on CT with the addition of calcium ions into the functionalization solution compared to the other cases. A more positive electric potential was registered on the functionalized area than the substrate only in the case of CT\_P\_Ca. In general,

adsorbates that donate electron density to the surface cause a decrease in surface potential, while adsorbates that pull electrons away from the surface cause an increase in surface potential [34]. Areas with a more positive surface potential can derive from either a more positive charge contribution from cations and/or less electron density from anions or negatively charged groups [35]. Thus, the increment of electric potential on the functionalized area of CT with the calcium ions added could be ascribed to the presence of adsorbed calcium ions. This hypothesis was confirmed by a similar increment of surface electric potential registered on an area of a CT sample soaked in a buffered solution of calcium chloride (without polyphenols) compared to the unsoaked area of the same specimen (data not shown). It could be also supposed that the polyphenols adsorbed on CT\_P\_Ca made a shield effect masking the negatively charged OH groups of the CT substrate resulting in a less negative surface electric potential. This effect was not observed on CT\_P because of the lower thickness of the adsorbed layer of polyphenols. These hypotheses are not convincing in the authors' opinion.

Despite the different chemical bonding mechanisms, with or without the addition of calcium ions, polyphenols formed a continuous layer on all surfaces, as can be concluded by combining the results of fluorescent microscopy and KPFM (Figures 2 and 3). These results were agreed in the case of Ti64\_P\_Ca, CT\_P, and CT\_P\_Ca. The homogeneous value of the electric potential detected by KPFM on Ti64\_P evidenced that a thin uniform layer of adsorbed molecules was formed also on this sample, analogously to the other ones, even if it was not observed in the fluorescent image. It can be supposed that it was too thin to result in a visible fluorescent contrast. Few fluorescence spots on a dark substrate were observed on Ti64\_P suggesting that polyphenols formed also aggregates on this sample; this agreed with the lower solubility of polyphenols in a solution without calcium ions. The hypothesis of a continuous polyphenol layer on Ti64\_P samples is also supported by the water contact angle being equal to one of Ti64\_P\_Ca as the result of similar surface chemistry between surfaces. On the other side, it was clear from the fluorescence images that both the addition of calcium ions to the functionalization solution and the presence of acidic OH groups on the substrate, as it was on CT, enhanced polyphenols adsorption. The highest amount of molecules was observed when both the effects of calcium took place (CT\_P\_Ca), while the lowest was obtained when both were absent (Ti64\_P). This effect is of interest for several applications of polyphenols where a uniform coating of a metal substrate is needed, such as protection against corrosion.

However, the thickness of the adsorbed polyphenols layer was at the nanoscale in any case, as derived by the KPFM topographical images (Figure 3) where the typical surface morphologies of Ti64 and CT were well visible even after functionalization on all samples. This agreed with the detection of titanium by XPS on all the functionalized surfaces: the thickness of the adsorbed layer was lower than the penetration depth of the beam used for the XPS measurements, which is a few nanometers. This is of interest considering that a micro and nano-structured topography, as in the case of CT, has a large osteoconductive effect and it must be exposed to the biological environment.

Concerning the evaluation of the stability at pH 4 and 7.4 of the functionalized surfaces through the zeta potential measurement at a constant pH, all the surfaces showed a stable behavior and no substantial change in the zeta potential value (Figure 6c,d). It can be concluded that at least a layer of polyphenols was not removed from the titanium surfaces by the electrolyte flux during zeta potential measurements, despite the type of chemical bond with the surface. This result agreed with what was reported by the author in [9] where a weak and uniformly distributed molecule layer was detected even on a sample soaked for 28 days in a simulated physiological solution. On the other side, the presence of a chemisorption mechanism could be related to the abrupt change in the zeta potential value registered at pH 4.5 on CT\_P\_Ca, as already described in [9], where polyphenols are released following the protonation of substrate's aCOH groups. The XPS data obtained on the samples used for the zeta potential titration in the acidic range (Figure 1–Tables 1 and 2; Ti64\_P\_Ca\_pza and CT\_P\_Ca\_pza) confirmed that a partial removal occurred during the

measures: the percentages of carbon decreased, while those of titanium and oxygen increased, and the contribution of the Ti-O bond was larger than on Ti64\_P\_Ca and CT\_P\_Ca. Furthermore, the amount of Ca was reduced on CT\_P\_Ca\_pza. A larger removal of the adsorbed polyphenols may occur on CT\_P\_Ca in a limited range of time and it took place at a specific pH that is of interest because reachable in inflammatory conditions. A smart release of polyphenols, when an inflammatory chemical environment is developed around an implant, as well as their persistent presence on an implant surface is of interest because of their well-known anti-inflammatory action [14,19]. The «smart» release of polyphenols occurred at a pH value that was consistent with the complete protonation of hydroxyl groups of the substrate according to the zeta potential titration curve of CT.

## 5. Conclusions

The present paper provides new insights into the chemical mechanisms of binding natural molecules for therapeutic purposes on biomaterials. A natural extract of grape pomace was used to functionalize Ti6Al4V alloy. The polished and chemically etched surfaces were compared as well as different solutions for functionalization. The amount and mechanism of adsorption of polyphenols were affected both by the presence of calcium ions in the solution used for functionalization and the surface features of the substrate. The amount of adsorbed polyphenols increased with the addition of calcium ions and the formation of complex compounds in the solution. The presence of acidic hydroxyl groups on the substrate had a positive effect on the adsorption of the polyphenols changing the mechanism from physisorption to chemisorption through electrostatic bridging and making desorption sensitive to pH. A selection of the types of polyphenols adsorbed occurred as a consequence of the surface features and addition of calcium ions to the solution used for functionalization. The novel functionalization with the natural extract may promote new smart materials for implants designed not only for bone regeneration but also for inflammation reduction.

**Author Contributions:** Conceptualization, S.F. and S.S.; Methodology, J.B., S.F. and S.S.; Investigation, C.R. and J.B.; Writing—original draft, C.R.; Writing—review and editing, J.B., S.F. and S.S.; Supervision, S.S.; Project administration, S.S.; Funding acquisition, S.S. All authors have read and agreed to the published version of the manuscript.

**Funding:** European Commission and Ministero dell'Università e della Ricerca (Italy) funded NAT4MORE (M.ERA-NET 2016—agreement no. 169010-0613).

**Data Availability Statement:** Not applicable.

**Acknowledgments:** CREA is acknowledged for the chemical analysis of natural extract. Politecnico di Torino is acknowledged for supporting open-access publication.

**Conflicts of Interest:** The authors declare no conflict of interest.

## References

1. Yamaguchi, M.; Spriano, S.; Cazzola, S. Nanostructured Biomaterials for Regenerative Medicine. *Curr. Nanosci.* **2019**, *2*, 155–177.
2. Falentin-Daudre, C. Functionalization of Biomaterials and Applications. *Biomaterials* **2014**, 119–133. [[CrossRef](#)]
3. Ferraris, S.; Vitale, A.; Bertone, E.; Guastella, S.; Cassinelli, C.; Pan, J.; Spriano, S. Multifunctional commercially pure titanium for the improvement of bone integration: Multiscale topography, wettability, corrosion resistance and biological functionalization. *Mater. Sci. Eng. C* **2016**, *60*, 384–393. [[CrossRef](#)]
4. Teixeira, G.T.L.; Nascimento, J.P.L.D.; Gelamo, R.V.; Moreto, J.A.; Slade, N.B.L. Strategies for Functionalization of Metallic Surfaces with Bioactive Peptides: A Mini Review. *Int. J. Pept. Res. Ther.* **2023**, *29*, 24. [[CrossRef](#)]
5. Daglia, M. Polyphenols as antimicrobial agents. *Curr. Opin. Biotechnol.* **2012**, *23*, 174–181. [[CrossRef](#)] [[PubMed](#)]
6. Jin, P.; Wu, H.; Xu, G.; Zheng, L.; Zhao, J. Epigallocatechin-3-gallate (EGCG) as a pro-osteogenic agent to enhance osteogenic differentiation of mesenchymal stem cells from human bone marrow: An in vitro study. *Cell Tissue Res.* **2014**, *356*, 381–390. [[CrossRef](#)]
7. Nanci, A.; Peru, L.; Brunet, P.; Sharma, V.; Zalzal, S.; McKee, M.D. Chemical modification of titanium surfaces for covalent attachment of biological molecules. *J. Biomed. Mater. Res.* **1998**, *40*, 324–335. [[CrossRef](#)]

8. Souza, J.C.M.; Sordi, M.B.; Kanazawa, M.; Ravindran, S.; Henriques, B.; Silva, F.S.; Aparicio, C.; Cooper, L.F. Nano-scale modification of titanium implant surfaces to enhance osseointegration. *Acta Biomater.* **2019**, *94*, 112–131. [[CrossRef](#)]
9. Riccucci, G.; Cazzola, M.; Ferraris, S.; Gobbo, V.A.; Guaita, M.; Spriano, S. Surface functionalization of Ti6Al4V with an extract of polyphenols from red grape pomace. *Mater. Des.* **2021**, *206*, 109776. [[CrossRef](#)]
10. Riccucci, G.; Cazzola, M.; Ferraris, S.; Gobbo, V.A.; Miola, M.; Bosso, A.; Örlýgsson, G.; Ng, C.H.; Verné, E.; Spriano, S. Surface functionalization of bioactive glasses and hydroxyapatite with polyphenols from organic red grape pomace. *J. Am. Ceram. Soc.* **2022**, *105*, 1697–1710. [[CrossRef](#)]
11. Ferraris, S.; Pan, G.; Venturello, A.; Bianchi, C.L.; Chiesa, R.; Faga, M.G.; Maina, G.; Verné, E. Surface modification of Ti-6Al-4V alloy for biomineralization and specific biological response: Part I, inorganic modification. *J. Mater. Sci. Mater. Med.* **2011**, *22*, 533–545. [[CrossRef](#)]
12. Spriano, S.F.S.; Verné, E. Multifunctional titanium surfaces for bone integration. EP2214732B1, 15 May 2013. Available online: <https://patents.google.com/patent/EP2214732B1/en> (accessed on 23 July 2023).
13. Liang, H.; Zhou, B.; Wu, D.; Li, J.; Li, B. Supramolecular design and applications of polyphenol-based architecture: A review. *Adv. Colloid. Interface Sci.* **2019**, *272*, 102019. [[CrossRef](#)] [[PubMed](#)]
14. Riccucci, G.; Ferraris, S.; Reggio, C.; Bosso, A.; Örlýgsson, G.; Ng, C.H.; Spriano, S. Polyphenols from Grape Pomace: Functionalization of Chitosan-Coated Hydroxyapatite for Modulated Swelling and Release of Polyphenols. *Langmuir* **2021**, *37*, 14793–14804. [[CrossRef](#)]
15. Evans, S. Correction for the effects of adventitious carbon overlayers in quantitative XPS analysis. *Surf. Interface Anal.* **1997**, *25*, 924–930. [[CrossRef](#)]
16. Fairley, N.; Fernandez, V.; Plouet, M.R.; Deudon, C.G.; Walton, J.; Smith, E.; Flahaut, D.; Greiner, M.; Biesinger, M.; Tougaard, S.; et al. Systematic and collaborative approach to problem solving using X-ray photoelectron spectroscopy. *Appl. Surf. Sci. Adv.* **2021**, *5*, 100112. [[CrossRef](#)]
17. Xps, T. XPS Spectra. \*, CasaXPS Copyright © 2013. Casa Software Ltd. pp. 1–77. Available online: [www.casaxps.com](http://www.casaxps.com) (accessed on 23 July 2023).
18. Barberi, J.; Mandrile, L.; Giovannozzi, A.M.; Miola, M.; Napione, L.; Rossi, A.M.; Vitale, A.; Yamaguchi, S.; Spriano, S. Effect on albumin and fibronectin adsorption of silver doping via ionic exchange of a silica-based bioactive glass. *Ceram Int.* **2023**, *49*, 13728–13741. [[CrossRef](#)]
19. Torino, P.D.I.; Gamna, F.; Yamaguchi, S.; Cochis, A.; Ferraris, S.; Kumar, A.; Rimondini, L.; Spriano, S. Conferring Antioxidant Activity to an Antibacterial and Bioactive Titanium Surface through the Grafting of a Natural Extract. *Nanomaterials* **2023**, *13*, 479.
20. Barberi, J.; Ferraris, S.; Giovannozzi, A.M.; Mandrile, L.; Piatti, E.; Rossi, A.M.; Spriano, S. Advanced characterization of albumin adsorption on a chemically treated surface for osseointegration: An innovative experimental approach. *Mater. Des.* **2022**, *218*, 110712. [[CrossRef](#)]
21. Nečas, D.; Klapetek, P. Gwyddion: An open-source software for SPM data analysis. *Open Phys.* **2012**, *10*, 181–188. [[CrossRef](#)]
22. Ferraris, S.; Yamaguchi, S.; Barbani, N.; Cazzola, M.; Cristallini, C.; Miola, M.; Verné, E.; Spriano, S. Bioactive materials: In vitro investigation of different mechanisms of hydroxyapatite precipitation. *Acta Biomater.* **2020**, *102*, 468–480. [[CrossRef](#)]
23. Cazzola, M.; Ferraris, S.; Boschetto, F.; Rondinella, A.; Marin, E.; Zhu, W.; Pezzotti, G.; Verné, E.; Spriano, S. Green tea polyphenols coupled with a bioactive titanium alloy surface: In vitro characterization of osteoinductive behavior through a KUSA A1 cell study. *Int. J. Mol. Sci.* **2018**, *19*, 2255. [[CrossRef](#)]
24. Neo, Y.P.; Swift, S.; Ray, S.; Gizdavic-Nikolaidis, M.; Jin, J.; Conrad, Perera, O. Evaluation of gallic acid loaded zein sub-micron electrospun fibre mats as novel active packaging materials. *Food Chem.* **2013**, *141*, 3192–3200. [[CrossRef](#)]
25. Ferraris, S.; Cazzola, M.; Peretti, V.; Stella, B.; Spriano, S. Zeta potential measurements on solid surfaces for in Vitro biomaterials testing: Surface charge, reactivity upon contact with fluids and protein absorption. *Front. Bioeng. Biotechnol.* **2018**, *6*, 60. [[CrossRef](#)] [[PubMed](#)]
26. Ferraris, S.; Cochis, A.; Cazzola, M.; Tortello, M.; Scalia, A.; Spriano, S.; Rimondini, L. Cytocompatible and Anti-bacterial Adhesion Nanotextured Titanium Oxide Layer on Titanium Surfaces for Dental and Orthopedic Implants. *Front. Bioeng. Biotechnol.* **2019**, *7*, 103. [[CrossRef](#)] [[PubMed](#)]
27. Barberi, J.; Mandrile, L.; Napione, L.; Giovannozzi, A.M.; Rossi, A.M.; Vitale, A.; Yamaguchi, S.; Spriano, S. Albumin and fibronectin adsorption on treated titanium surfaces for osseointegration: An advanced investigation. *Appl. Surf. Sci.* **2022**, *599*, 154023. [[CrossRef](#)]
28. Metwally, S.; Ferraris, S.; Spriano, S.; Krysiak, Z.J.; Kaniuk, Ł.; Marzec, M.M.; Kim, S.K.; Szewczyk, P.K.; Gruszczyn, A.; Wytrwal-Sarna, M.; et al. Surface potential and roughness controlled cell adhesion and collagen formation in electrospun PCL fibers for bone regeneration. *Mater. Des.* **2020**, *194*, 108915. [[CrossRef](#)]
29. Scannavino, R.C.P.; Riccucci, G.; Ferraris, S.; Duarte, G.L.C.; de Oliveira, P.T.; Spriano, S. Functionalization with Polyphenols of a Nano-Textured Ti Surface through a High-Amino Acid Medium: A Chemical-Physical and Biological Characterization. *Nanomaterials* **2022**, *12*, 2916. [[CrossRef](#)]
30. Mera, A.C.; Contreras, D.; Escalona, N.; Mansilla, H.D. BiOI microspheres for photocatalytic degradation of gallic acid. *J. Photochem. Photobiol. A Chem.* **2016**, *318*, 71–76. [[CrossRef](#)]
31. Cazzola, M.; Ferraris, S.; Prenesti, E.; Casalegno, V.; Spriano, S. Grafting of gallic acid onto a bioactive Ti6Al4V alloy: A physico-chemical characterization. *Coatings* **2019**, *9*, 302. [[CrossRef](#)]



32. Ferraris, S.; Perero, S.; Costa, P.; di Confiengo, G.G.; Cochis, A.; Rimondini, L.; Renaux, F.; Vernè, E.; Ferraris, M.; Spriano, S. Antibacterial inorganic coatings on metallic surfaces for temporary fixation devices. *Appl. Surf. Sci.* **2020**, *508*, 144707. [[CrossRef](#)]
33. Hori, N.; Ueno, T.; Minamikawa, H.; Iwasa, F.; Yoshino, F.; Kimoto, K.; Lee, M.C.-I.; Ogawa, T. Electrostatic control of protein adsorption on UV-photofunctionalized titanium. *Acta Biomater.* **2010**, *6*, 4175–4180. [[CrossRef](#)] [[PubMed](#)]
34. Walker, S.M.; Marcano, M.C.; Kim, S.; Taylor, S.D.; Becker, U. Understanding Calcite Wettability Alteration through Surface Potential Measurements and Molecular Simulations. *J. Phys. Chem. C* **2017**, *121*, 28017–28030. [[CrossRef](#)]
35. Long, X.; Wang, X.; Yao, L.; Lin, S.; Zhang, J.; Weng, W.; Cheng, K.; Wang, H.; Lin, J. Graphene/Si-Promoted Osteogenic Differentiation of BMSCs through Light Illumination. *ACS Appl. Mater. Interfaces* **2019**, *11*, 43857–43864. [[CrossRef](#)] [[PubMed](#)]

**Disclaimer/Publisher’s Note:** The statements, opinions and data contained in all publications are solely those of the individual author(s) and contributor(s) and not of MDPI and/or the editor(s). MDPI and/or the editor(s) disclaim responsibility for any injury to people or property resulting from any ideas, methods, instructions or products referred to in the content.